Journal of Ceramic Processing Research. Vol. 20, No. 3, pp. 280~285 (2019)
(Received 15 November 2018, Received in revised form 7 February 2019, Accepted 9 May 2019)

J O U R N A L O F
Ceramic Processing Research

Scintillation properties of $GdAlO_3$ single crystals doped with Nd

M. Akatsuka*, N. Kawaguchi and T. Yanagida
Graduate School of Materials Science, Nara Institute of Science and Technology, 8916-5 Takayama, Ikoma, Nara 630-0192, Japan

Nd-doped $GdAlO_3$ single crystals were synthesized by the floating-zone method to evaluate their scintillation properties, particularly in the near-infrared (NIR) range. Under X-ray irradiation, scintillation due to the $^4F_{3/2}\rightarrow{}^4I_{11/2}$ transition of Nd^{3+} was observed at 1064 nm. By changing the irradiation dose from 1 mGy-10Gy, we evaluated the relation between the scintillation intensity and the X-ray dose, and some samples showed good linearity. The scintillation decay time ranged 66-241 μs due to Nd^{3+}.

Key words: Scintillation, Near-infrared, Nd, Perovskite.

Introduction

Scintillators are a kind of phosphor materials which have a function to convert the ionizing radiation (e.g. γ-rays, α-rays) to thousands of low-energy photons such as ultraviolet and visible light [1, 2]. They are used in various different fields; for examples, medical imaging [3], security [4], environmental monitoring [5] and high-energy physics [6]. The scintillation properties are affected by materials forms such as inorganic/organic solid, liquid and gas. Among them, inorganic solid-state scintillators are easily handled so radiation detectors with inorganic scintillators are the most common among all the types of detectors. The basic requirements for the scintillator are a high light yields, a fast decay, a high density, a large effective atomic number, a chemical stability, and a radiation hardness [2, 7]. In reality, there is no perfect scintillator which fulfills all the properties required for all the applications. Therefore, we select suitable scintillators for their purposes.

Generally, scintillators are used with photomultiplier tube (PMT). The scintillator can convert the ionizing radiation to thousands of low-energy photons, and these photons are converted to electrons by PMT via the photoelectric conversion. Because the spectral sensitivity range of PMTs is generally 250-600 nm, conventional scintillators emitting ultraviolet (UV) or visible (VIS) light have been developed. On the other hand, semiconductor type photodetectors such as a photodiode are developed and near-infrared (NIR) photons become detectable. Therefore scintillators emitting NIR photons are being studied in recent years. Scintillators emitting NIR photons have attracted much attention because NIR photons have unique characteristics such as a high penetration power without a fatal damage to a human body [8-12]. Since an optical window is from 700–1200 nm in the human body, the scintillator materials emitting NIR photons can be applied for radiation-based bio imaging applications [13, 14]. For example, in radiation therapy, a real time monitoring of irradiation dose at affected parts will be possible by bio imaging based techniques. In such application, if a very small size of NIR emitting scintillator is embedded in the affected part of the human body, NIR scintillation can be detected outside the body during the irradiation.

In addition, in high-dose environments (e.g., nuclear reactor), such NIR emitting scintillators are expected to be an effective tool for monitoring dose. High-dose environments generates Cherenkov radiation from detectors such as an optical fiber in the UV~blue range. The wavelength of Cherenkov photons overlap with the scintillation signal if the scintillation emission wavelength is in the UV-blue, and they cause incorrectness radiation measurements. In this case, scintillators emitting NIR photons are advantageous so that scintillation signal is easily distinguished from the Cherenkov noise. Moreover, scintillation detector which monitors high radiation dose are used combined scintillator and optical fiber in general. The optical transmittance of UV-VIS wavelength is degraded by high dose [15], which weakens signals detected by photodetectors. On the other hand, degradation of transmittance in the NIR range is much smaller, so NIR-emitting scintillators are suitability in such a high-dose environment.

However, in spite of such usefulness as above, there have been only a few reports on NIR-emitting scintillators, and there remains much room for studying on this topic.

*Corresponding author:
Tel : +81-743-72-6144
E-mail: akastuka.masaki.ad5@ms.naist.jp

One reason is that the detection of NIR scintillation is technically difficult when the conventional Si-based photodetectors are used. The conventional Si-based photodetectors are sensitive to light of wavelengths shorter than 800 nm, so in previous studies, only emissions up to 800 nm could be characterized [16, 17]. Recently, we have dramatically expanded the spectral range of measurement by using an InGaAs-based detector, and we have been studying NIR-emitting scintillators for bio-imaging and the high-dose monitoring applications. Up to now, NIR scintillations (600-1650 nm) in sesquioxides (Yb^{3+} added Lu_2O_3), fluorides (Nd^{3+} doped $YLiF_4$), and oxide garnets (emission center is Nd^{3+}) have been reported [18-22].

In order to expand the research on scintillators emitting NIR photons, in this study, we synthesized Nd-doped $GdAlO_3$ single crystals by floating-zone (FZ) method and then evaluated the photoluminescence (PL), and scintillation properties. Since rare earth doped $GdAlO_3$:R (R=Ce, Eu, Tb, Dy, Er, and Yb) exhibit high density, chemical and thermal stability, and unique electronic and spectroscopic properties, their photoluminescence and scintillation properties have been already studied [23-26]. However, Scintillation properties of Nd-doped $GdAlO_3$ have not been studied yet.

Experiment

Nd-doped $GdAlO_3$ (Nd = 0.1, 0.3, 1.0, 3.0, 10 mol%) samples were synthesized by the FZ method. Nd was added with respect to gadolinium. The raw material powders were Gd_2O_3 (4N), Al_2O_3 (4N), and Nd_2O_3 (4N), and they were mixed to the compositions as above. After mixing, powders were formed to a cylindrical rod by applying hydrostatic pressure. Then, the cylinders of all the compositions were sintered at 1100 °C for 8 hours in air to obtain ceramic rods. Finally, we conducted the crystal growth by melting the ceramic rod via the FZ method in air. The FZ furnace used here was Canon Machinery FZD0192. During the crystal growth, the rotation rate was about 20 rpm, and the pull-down rate was about 4 mm/h.

To evaluate the obtained crystalline phase, the X-ray diffraction (XRD) patterns were measured by a diffractometer (MiniFlex600, Rigaku) over a 2θ range of 10-90 degrees. A Cu (Kα) X-ray tube was used as the X-ray source, and the tube voltage and current were 40 kV and 15 mA, respectively.

The PL excitation/emission contour spectrum (or PL map) and PL quantum yield (*QY*) were measured using Quantaurus-QY (C11347, Hamamatsu). The excitation and emission wavelength ranges for the PL map were 250-800 and 300-950 nm, respectively. PL decay time profiles were evaluated using Quantaurus-τ (C11367, Hamamatsu), and the excitation and monitoring wavelengths were selected on the basis of the obtained PL contour map.

The scintillation spectra were evaluated at room temperature under X-ray irradiation in our original set up [27]. The excitation source was an X-ray generator (XRB80N100, Spellman) equipped with a conventional X-ray tube, supplied with 60 kV bias voltage and 1.0 mA tube current. The emission spectra were measured using two different spectrometers to cover a wide spectral range from UV to NIR: Andor Newton 920 for 180-700 nm and Andor iDUS for 650-1650 nm. The CCDs of the Andor spectrometers were cooled to 188K using a Peltier device to reduce the thermal noise. In order to avoid the CCD exposed to X-rays directly, the spectrometer was placed off the irradiation axis, and the scintillation light was guided into the spectrometer through a 2 m optical fiber. Moreover, we measured the relation between the scintillation intensity and X-ray exposure doses in NIR wavelength from 1mGy-10Gy by controlling the tube current and the irradiation distance in order to evaluate the detector property. The scintillation decay time profiles by X-ray irradiation were evaluated by using an afterglow characterization system equipped with a pulse X-ray tube [28]. The system is commercially available from Hamamtsu Photonics as a custom-ordered instrument. The applied voltage to the pulse X-ray source was 30 kV, and the system offers the timing resolution of ~1 ns.

Result and Discussion

Sample appearance

As-synthesized rods were typically 4 mm in diameter and 15-20 mm in length. These rods were cut in to pieces for characterization. Fig. 1 shows the samples used for the characterization. All the samples look transparent with some cracks. In addition the color of samples looked purple as the concentration of Nd increases. This fact demonstrates that the actual Nd concentration of synthesized single crystals was

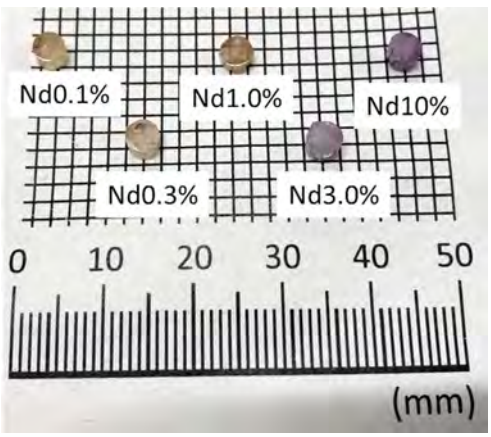

Fig. 1. Photograph of $GdAlO_3$ sample doped with different concentrations of Nd.

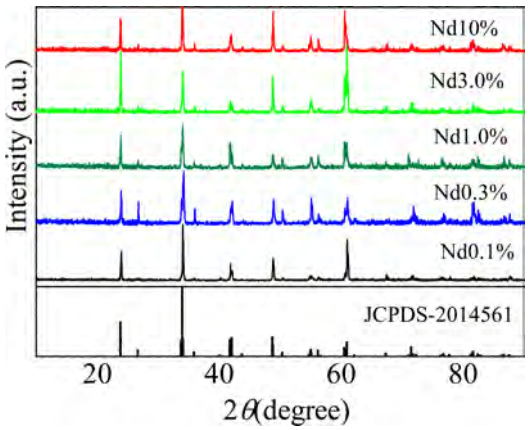

Fig. 2. Powder XRD patterns of $GdAlO_3$ doped with different concentrations of Nd.

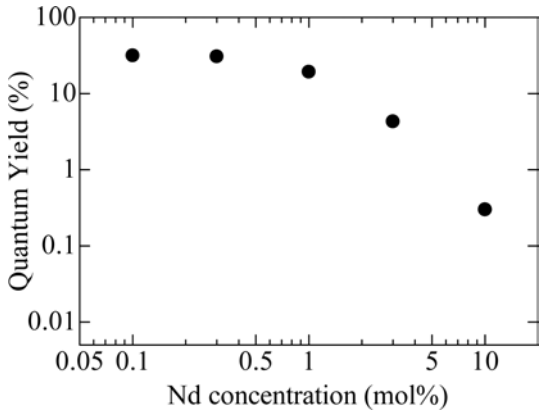

Fig. 4. *QY* plot of $GdAlO_3$ doped as a function of Nd concentrations. The horizontal and vertical axes show Nd concentrations and *QY*, respectively.

proportional to nominal concentration, although the segregation would occur.

Fig. 2 shows the powder XRD patterns of prepared samples. All the diffraction patterns corresponded well with the standard crystallographic data (JCPDS nos. 2014561). The all the samples seems to have a perovskite single-crystal phase.

Photoluminescence properties

Fig. 3 shows the PL excitation and emission contour map of 0.1 % Nd-doped $GdAlO_3$ as a representative example. It shows a strong emission around 900 nm owing to the 4f-4f transitions of Nd^{3+} [29]. Here, we integrated the signal intensity from 800 to 950 nm for all samples and calculated *QY* values, as shown in Fig. 4. As a result, *QY* values of Nd 0.1, 0.3, 1.0, 3.0, and 10.0 % samples were 31.6, 30.7, 19.3, 4.3, and 0.3 %, respectively. Among all the samples, the 0.1 % Nd-doped sample showed the highest *QY* value, and *QY* monotonically decreased with the Nd concentration. Furthermore, it can be seen from Fig. 4 that the *QY* rapidly decreases from the 1.0 % Nd-doped sample. We consider the concentration quenching arises around 1.0 % Nd concentration. The well-known intense emission of Nd^{3+} at 1064 nm is not included because our apparatus cannot measure photons of wavelength longer than 960 nm.

PL decay curves of all samples are illustrated in Fig. 5. Here, the monitoring wavelength was around 900 nm while the excitation wavelength was 575-625 nm. The excitation wavelengths were selected for the PL emission map. The decay curves of all the samples could be approximated by a single exponential decay functions. The obtained decay time constants were 12-207 μs. For the 0.1-3.0 % Nd-doped samples, the PL decay times are typical values of emission from 4f-4f transitions of Nd^{3+} and agreed with the values reported in past studies [29-31]. On the other hand, 10 % Nd-doped samples have very short decay time. This finding supports the idea that these samples suffered from concentration quenching. Moreover, the decay times of the 1.0 and 3.0 % Nd-doped sample were shorter than those of 0.1 and 0.3 % Nd-doped

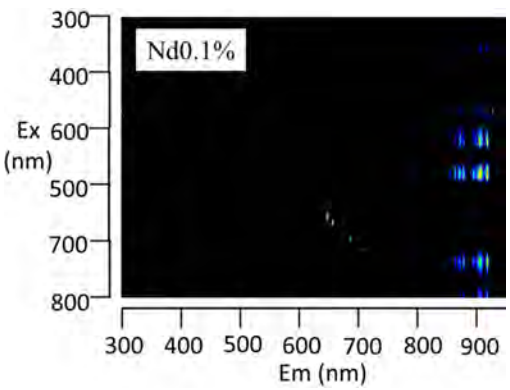

Fig. 3. PL contour map of 0.1 % Nd-doped $GdAlO_3$. The horizontal and vertical axes show emission and excitation wavelength, respectively.

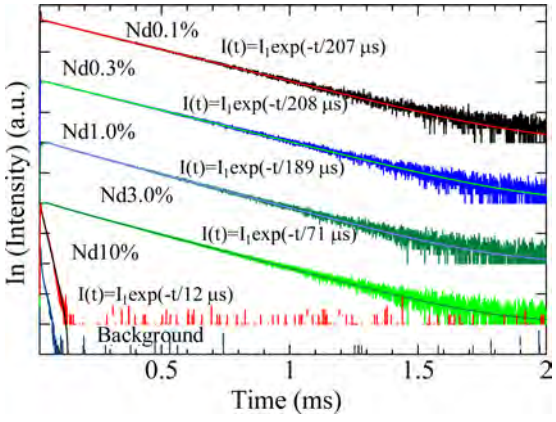

Fig. 5. PL decay curves of $GdAlO_3$ doped with different concentrations of Nd. The monitoring wavelength was around 900 nm.

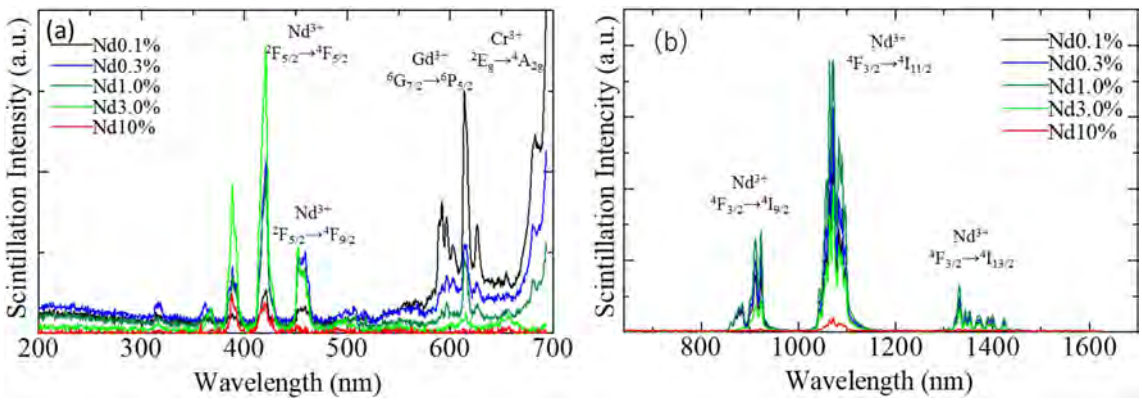

Fig. 6. X-ray-induced scintillation spectra of $GdAlO_3$ doped with different concentrations of Nd in the (a) UV-VIS and (b) NIR ranges.

samples. This tendency coincides with the result of *QY*.

Scintillation properties

Fig. 6 represents X-ray-induced scintillation spectra measured in the (a) UV-VIS and (b) NIR ranges. For the all samples, the various kinds of peaks were observed in the UV-VIS range, which were not observed in PL. Strong peaks can be identified as the electronic transitions of Nd^{3+} as: $^2F_{5/2}\rightarrow{}^4F_{5/2}$ (400 nm), $^2F_{5/2}\rightarrow{}^4F_{9/2}$ (450 nm). The emission peaks were consistent with typical spectrum due to the Nd^{3+} electronic transitions [18, 21, 32, 33]. The intensity of emission peak around 600 and 700 nm is decreased as Nd concentration decrease, and this phenomenon is different from the tendency around 400 and 450 nm. Therefore, we assume the origin of this emission around 600~700 is other than Nd^{3+}. We consider the emission peak around 600 nm is due to Gd^{3+} $^6G_{7/2}\rightarrow{}^6P_{7/2}$ [34] transition since Gd^{3+} is included as a host material, and the emission peak around 700 nm is due to a little contamination of Cr^{3+} $^2E_g\rightarrow{}^4A_{2g}$ [35] transition because to obtain Cr-free Al_2O_3 raw materials is difficult. In the NIR range, all the samples showed emissions due to the electronic transition of Nd^{3+} $^4F_{3/2}\rightarrow{}^4I_{9/2}$ (910 nm), $^4F_{3/2}\rightarrow{}^4I_{11/2}$ (1064 nm), and $^4F_{3/2}\rightarrow{}^4I_{13/2}$ (1320 nm). The emission of 1064 nm is well known for laser applications [36], and the emission of 0.1-3.0% Nd-doped samples were high. The emission of the 10% Nd-doped sample was very weak, which was consistent with the results of PL.

As a detector property, the relationship between the scintillation intensity and X-ray exposure dose from 1 mGy to 10 Gy in NIR wavelength are shown in Fig. 7. All samples showed approximately liner proportional relations. In addition, 0.1-3.0 Nd-doped samples indicated a high sensitivity with a dynamic range of at least 1 mGy to 10 Gy. This result exceeds the past studies both of lower and upper detection limits [21]. However, when considering practical application, the more improvement is necessary. For example, as one way to improve the emission intensity, the co-doping of Nd and Cr would be effective. Some previous reports indicated that the energy transfer was caused from Cr^{3+} to Nd^{3+}, and it gave enhancement to the NIR emission [37, 38].

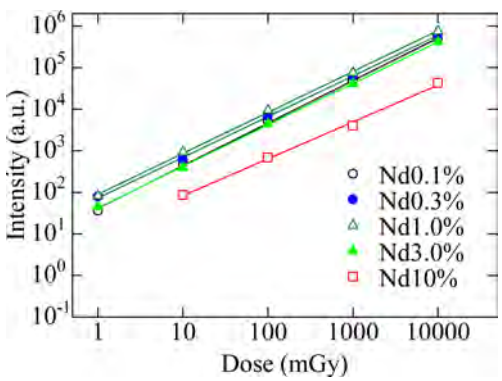

Fig. 7. The relation between the scintillation intensity and X-ray exposure dose from 1 mGy to 10 Gy in NIR wavelength of $GaAlO_3$ doped with concentration of Nd.

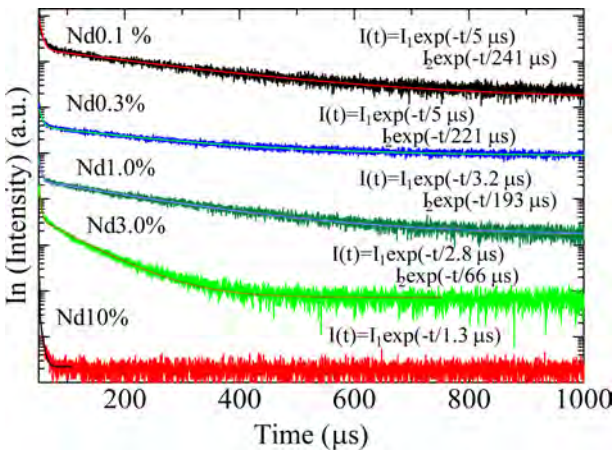

Fig. 8. X-ray-induced scintillation decay time profiles of $GdAlO_3$ doped with different concentrations of Nd. The monitoring wavelength was 400-900 nm.

Fig. 8 shows X-ray-induced scintillation decay time profiles of Nd-doped $GdAlO_3$. The decay curves of the 0.1-3.0% Nd-doped samples were approximated as a sum of two exponential decay functions, and the faster decay component was considered to be a tail of the instrumental response (~5 μs) in this time range while the longer component was considered to be the signal from the sample. These components were due to the 4f-4f transitions of Nd^{3+} and they were typical values of the 4f-4f transitions of Nd^{3+} reported from past studies [19-21]. In contrast, the 10 % Nd-doped sample was approximated by a single exponential decay function. The drastic decrease of the decay time in Nd 10% doped sample is considered that distance between Nd^{3+} ions became close and it suffered from the concentration quenching.

Conclusion

We synthesized Nd-doped $GdAlO_3$ by the FZ method to evaluate their PL and scintillation properties. In the PL contour graph, 0.1-0.3 % samples showed a strong peak emission around 900 nm due to the 4f-4f transitions of Nd^{3+}. The *QY* and PL decay times of 0.1-3.0 samples were 4.3-31.6 % and 71-208 μs, respectively. The 10 % Nd-doped sample suffered from the concentration quenching in PL. In the scintillation spectra, the 0.1-3.0 % Nd-doped samples demonstrated a strong emission peak at 1064 nm owing to $^4F_{3/2} \rightarrow {}^4I_{11/2}$ transitions of Nd^{3+}. The relation between the scintillation intensity and X-ray exposure dose from 1 mGy to 10 Gy in NIR wavelength was approximately liner. It was confirmed that Nd-doped $GdAlO_3$ worked as NIR emitting scintillator.

Acknowledgements

This work was supported by Grant-in-Aid for Scientific Research (A) (17H01375) and (B) (18H03468) from the Ministry of Education, Culture, Sports, Science and Technology of the Japanese government (MEXT) as well as A-STEP from Japan Science and Technology Agency (JST). The Cooperative Research Project of Research Institute of Electronics, Shizuoka University, Terumo Foundation for Life Sciences and Arts, Izumi Science and Technology Foundation, SEI Group CSR Foundation, The Kazuchika Okura Memorial Foundation, and The Iwatani Naoji Foundation are also acknowledged.

References

1. T. Yanagida, Proc. of the Japan Academy, B, 94 (2018) 75-97.
2. C. W. E. Eijk, Nucl. Instrum. Methods Phys. Res. Sect. A. 460, (2001) 1-14.
3. S. Yamamoto, K. Kuroda, M. Senda, IEEE Trans. Nucl. Sci., 50, (2003) 1683-1685.
4. J. Glodo, Y. Wang, R. Shawgo, C. Brecher, R. H. Hawrami, J. Tower, K. S. Shah, Phys. Procedia, 90 (2017) 285-290.
5. S. Moriuchi, M. Tsutsumi, K. Saito, Jpn. J. Heal. Phys. 42 (2007) 71-83.
6. T. Ito, T.Yanagida, M. Sato, M. Kokubun, T. Takashima, S. Hirakuri, R. Miyawaki, H. Takahashi, K. Makishima, T. Tanaka, K. Nakazawa, T. Takahashi, and T. Honda, A, Nucl. Instr. and Meth. A, 579 (2007) 239-242.
7. S. E. Derenzo, M. J. Weber, E. Bourret-Courchesne and M. K. Klintenberg, Nucl. Instrum. Methods Phys. Res. Sect. A. 505, (2003) 111-117.
8. Y. Huang, M. Hamblin, and A. C.-H. Chen: SPIE (2009) doi:10.1117/2.1200906.1669.
9. R. Weissleder, Nat. Biotechnol. 19 (2001) 316-317.
10. C. Amiot, S. Xu, S. Liang, L. Pan, and J. Zhao, Sens. 8 (2008) 3082-3105.
11. K. Soga, T. Tsuji, F. Tashiro, J. Chiba, M. Oishi, K. Yoshimoto, Y. Nagasaki, K. Kitano, and S. Hamaguchi, J. Phys.: Conf. Ser. 106 (2008) 012023.
12. J.-L. Boulnois, Lasers Med. Sci. 1 (1986) 47-66.
13. L. Sudheendra, G. K. Das, C. Li, D. Stark, J. Cena, S. Cherry, I. M. Kennedy, Chem. Mater. 26 (2014) 1881-1888.
14. G. Pratx, C. M. Carpenter, C. Sun, R. P. Rao, L. Xing, Opt. Lett. 35 (2010) 3345-3347.
15. K. Toh, T. Nakamura, H. Yamagishi, K. Sakasai, K. Soyama, T. Shikama, Nucl. Instrum. Methods A, 700 (2013) 130-134.
16. W. W. Moses, M. J. Weber, S. E. Derenzo, D. Perry, P. Berdahl, and L. A. Boatner: IEEE Trans. Nucl Sci. 45 (1998) 462-466.
17. P. A. Rodnyi, E. I. Gorohova, S. B. Mikhrin, A. N. Mishin, and A. S. Potapov, Nucl. Instrum. Methods A 486 (2002) 244-249.
18. T. Yanagida and H. Sato, Opt. Mater. 38 (2014) 174-178.
19. T. Yanagida, Y. Fujimoto, H. Yagi, and T. Yanagitani, Opt. Mater. 36 (2014) 1044-1048.
20. T. Yanagida, Y. Fujimoto, S. Ishizu, and K. Fukuda, Opt. Mater. 41 (2015) 36-40.
21. T. Oya, G. Okada, and T. Yanagida, J. Ceram. Soc. Jpn. 124 (2016) 536-540.
22. G. Okada, N. Kawaguchi, and T. Yanagida, Sens. Mater. 29 (2017) 1407-1415.
23. H.H.S. Oliveira, M.A. Cebim, A.A. Da Silva, and M.R. Davolos, J. Alloys Compd. 488 (2009) 619-623.
24. Y. Liu, X. Tong, F. Lai, X. Chen, and W. You, Physica B 406 (2011) 1272–1275.
25. G.S.R. Raju, J.Y. Park, H.C. Jung, B.K. Moon, J.H. Jeong, and J.H. Kim, Curr. Appl. Phys. 9 (2009) e92-e95
26. P. Dorenbos , E. Bougrine , J. T. M. De Haas, C. W. E. Van Eijk, and M. V. Korzhik, Radi. Effe. Defe. Soli. 135 (1995) 321-323.
27. T. Yanagida, K. Kamada, Y. Fujimoto, H. Yagi, and T. Yanagitani, Opt. Mater. 35 (2013) 2480-2485.
28. T. Yanagida, Y. Fujimoto, T. Ito, K. Uchiyama, and K. Mori, Appl. Phys. Exp. **7** (2014) 062401.
29. H. S. Möller, A. Hoffmann, D. Knaut, J. Flottmann, and T. Jüstel, J. Lumin. 158 (2015) 365-370.
30. H. Yagi, T. Yanagitani, K. Takaichi, K. Ueda, and A. A. Kaminskii, Opt. Mater. 29 (2007) 1258-1262.
31. J. Lu, M. Prabhu, J. Song, C. Li, J. Xu, K. Ueda, A. A. Kaminskii, H. Yagi, and T. Yanagitani, Appl. Phys. B 71 (2000) 469-473.
32. S. M. Reda, C.R. Varney, and F.A. Selim, Res. Phys. 2 (2012) 123-126.

33. L. Ninga, P. A. Tannera, V. V. Harutunyanb, E. Aleksanyan, V. N. Makhov, and M. Kirm, J. Lumin., 127 (2007) 397-403.
34. R. T. Wegh, H. Donker, and A. Meijerink, Phys. Review B 56 (1997) 841-847.
35. H. B. Premkumar, D. V. Sunitha, H. Nagabhushana, S. C. Sharma, B. M. Nagabhushana, J. L. Rao, K. Gupta, R. P. S. Chakradhar: Spectro. Acta Part A: Mole. Biomole. Spectroscopy 96 (2012) 154-162.
36. X. D. Xu, X. D. Wang, J. Q. Meng, Y. Cheng, D. Z. Li, S. S. Cheng, F. Wu, Z. W. Zhao, and J. Xu, Laser Phys. Lett. 6 (2009) 678.
37. J. A. Mares, W. Nie, G. Boulon, J. Phys. Frances 51 (1990) 1655-1669.
38. E. Luria, S. R. Rotman, J. A. Mares, G. Boulon, A. Brenier, L. Lou, J. Lumin. 72-74 (1997) 951-953.